Design Comparison of Four-Layer Full-Nb_3Sn and Hybrid Nb_3Sn/NbTi Cos-Theta Dipoles for the CERN High Field Magnet R&D Programme

M. Elisei, E. Beneduce, A. Bersani, M. Bracco, S. Burioli, B. Caiffi, M. Cannavò, G. Crespi, E. De Matteis, S. Dotti, S. Farinon, A.P. Foussat, A. Gagno, T. Maiello, S. Mariotto, R. Musenich, D. Novelli, A. Pampaloni, M. Prioli, L. Rossi, *Fellow, IEEE*, N. Sala, C. Santini, M. Sorbi, S. Sorti, M. Spadotto, M. Statera, E. Todesco, and R.U. Valente

***Abstract*—The High Field Magnet (HFM) R&D programme at CERN aims to find technological solutions for the construction of accelerator magnets to be installed in future post-LHC colliders. The Italian Institute for Nuclear Physics (INFN) and CERN are collaborating to design and fabricate a new four-layer cos-theta dipole able to achieve a bore field of 14T with at least 20% margin on the load-line. Two design options are under evaluation: a four-layer dipole entirely made of Nb_3Sn, and a hybrid configuration combining inner Nb_3Sn layers with outer NbTi layers. Both options are being assessed for feasibility as short models, with scalable design choices for longer magnet prototypes suitable for accelerator integration. This paper presents a comparative study of the performance of the two design options. The results provide insights into the trade-offs between performance, complexity, and protection constraints in the development of next-generation high-field dipole magnets. The Full-Nb_3Sn solution satisfies the HFM requirements, but the Hybrid solution is a promising, cost-effective alternative that can be considered for next-generation colliders.**

***Index Terms*—Accelerator magnets, dipoles, Nb_3Sn, NbTi.**

Received 28 July 2025; revised 10 September 2025; accepted 22 September 2025. Date of publication 1 October 2025; date of current version 14 October 2025. This work was supported by NextGeneration EU- Italian National Recovery and Resilience Plan, Mission 4 - Component 2 - Investment 3.1. - Project name: IRIS, under Grant CUP: I43C21000230006. *(Corresponding author: M. Elisei.)*

M. Elisei is with the Università degli Studi di Roma "La Sapienza", 00185 Roma, Italy, and also with I.N.F.N., Laboratorio Acceleratori e Superconduttività Applicata, 20090 Milano, Italy (e-mail: mattia.elisei@mi.infn.it).

E. Beneduce, M. Cannavò, S. Mariotto, L. Rossi, M. Sorbi, and S. Sorti are with the Università degli Studi di Milano, 20122 Milano, Italy, and also with I.N.F.N., Laboratorio Acceleratori e Superconduttività Applicata, 20090 Milano, Italy.

A. Bersani, S. Burioli, B. Caiffi, S. Farinon, A. Gagno, T. Maiello, R. Musenich, and A. Pampaloni are with the I.N.F.N. Sezione di Genova, 16146 Genova, Italy.

M. Bracco is with the Università degli Studi di Genova, 16146 Genova, Italy, and also with I.N.F.N. Sezione di Genova, 16146 Genova, Italy.

G. Crespi, E. De Matteis, S. Dotti, M. Prioli, C. Santini, M. Statera, and R.U. Valente are with I.N.F.N., Laboratorio Acceleratori e Superconduttività Applicata, 20090 Milano, Italy (e-mail: riccardo.valente@mi.infn.it).

A.P. Foussat, N. Sala, and E. Todesco are with the European Organization for Nuclear Research, 1211 Geneva, Switzerland.

D. Novelli is with the Università degli Studi di Roma "La Sapienza", 00185 Roma, Italy, and also with I.N.F.N. Sezione di Genova, 16146 Genova, Italy.

M. Spadotto is with the Politecnico di Milano, 20133, Milan, Italy, and also with I.N.F.N., Laboratorio Acceleratori e Superconduttività Applicata, 20090 Milano, Italy.

Color versions of one or more figures in this article are available at https://doi.org/10.1109/TASC.2025.3615181.

Digital Object Identifier 10.1109/TASC.2025.3615181

I. Introduction

THE continuous push for higher energy frontiers in particle physics necessitates the development of next-generation accelerator magnets capable of producing magnetic fields significantly stronger than those currently achieved at the Large Hadron Collider (LHC) [1]. While the cos-theta layout has proven to be a reliable and well-established architecture for generating high-quality accelerator fields, the community is actively exploring alternative coil configurations—such as block-coil [2], common-coil [3], [4], canted cosine-theta [5] and stress-management cosine-theta [6] designs—to address the increasing mechanical and manufacturing challenges associated with high-field magnet technologies. In the context of the High Field Magnet (HFM) programme [7], [8], the primary objective is to validate a magnet design capable of reaching a nominal bore field of 14 T within a 50 mm aperture, while maintaining a minimum 20% operating margin on the load-line. This paper presents and compares two distinct magnet designs developed within the HFM framework: a four-layer Full-Nb_3Sn configuration and a four-layer Hybrid Nb_3Sn/NbTi configuration. Both designs were developed starting from the selection of the superconducting cable, which significantly influences not only the electromagnetic performance but also the mechanical and thermal behaviour of the final magnet. In contrast to the previous design [9], the strand diameter has been reduced from 1.1 mm to 0.85 mm while maintaining the same number of strands. This reduction in strand diameter is intended to facilitate the winding process, as experience from FALCON Dipole [10], [11], [12], [13], [14], [15], [16], [17], [18], [19], [20], [21] indicate that winding a 1 mm diameter strand with 40 strands around a 50 mm aperture is challenging. Moreover, the increased copper fraction helps with the magnet quench protection, and the finer filaments contribute to improve flux jump stability. It's crucial to note that these Nb_3Sn strands have already been extensively tested and validated in the context of the High-Luminosity LHC programme [22], thus providing a strong basis for reliability. Both designs aim to satisfy the

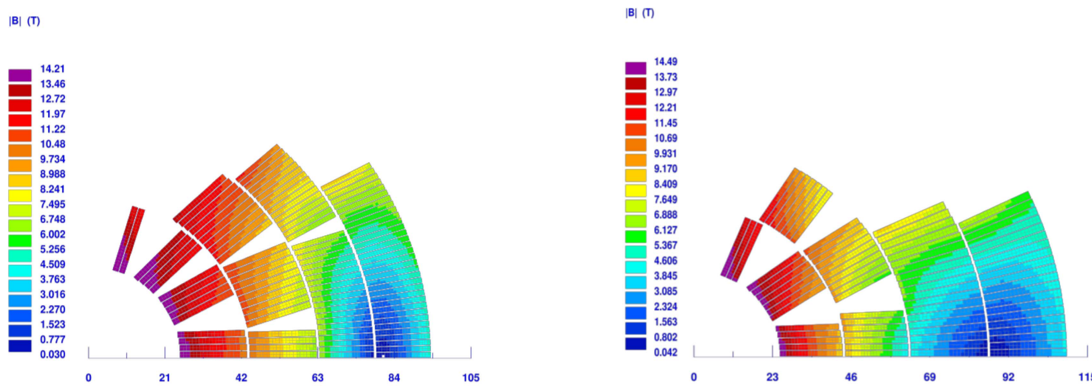

(a) Full-Nb_3Sn (b) Hybrid Nb_3Sn/NbTi

Fig. 1. Field distribution in one quadrant of each cross-section evaluated with the ROXIE software.

TABLE I
COMPARISON OF THE TWO DESIGNS

	Full Nb_3Sn				**Hybrid Nb_3Sn/NbTi**	
	HF 1.9K	**HF 4.2K**	**LF 1.9K**	**LF 4.2K**	**HF 1.9K**	**LF 1.9K**
Achieved bore field [T]	14				14	
Current [A]	9800				13330	
Peak field [T]	14.21		11.28		14.47	8.44
Current density [A/mm^2]	280		400		380	260
Supercond. current density [A/mm^2]	950		1400		1300	973
Copper current density [A/mm^2]	792		1167		1080	608
Loadline fraction [%]	80	87.5	73	80	86.5	78
Temperature margin [K]	4.4	2.2	5.6	3.3	3.28	2.28
Enthalpy margin [mJ/cm^3]	12.4	8.9	19.3	16	6.6	2.5
b_3 / b_5 / b_7 / b_9 at nominal [unit]	0.47 / -5.81 / 3.57 / 1.33				-0.98 / -0.93 / 4.29 / 2.94	
Equivalent width [mm]	55.4				59	
N° of turns (per pole)	39		69		39	39
N° blocks (per pole)	7		3		6	2
Aperture [mm]	50				50	
Maximum azimuthal stress [MPa]	83				116	
Maximum radial stress [MPa]	97				138	

requirements set by the HFM programme, but with different trade-offs.

II. FULL-Nb_3Sn DIPOLE

The first design option under consideration is a four-layer dipole made entirely of Nb_3Sn superconductor. As illustrated in Fig. 1(a), the coil is structured into two High-Field (HF) inner layers and two Low-Field (LF) outer layers. To optimize the use of the superconductor and manage costs, a "grading" approach has been implemented [23], [24]. This technique involves using different cables for each region, depending on the local magnetic field condition. The bare cable details are listed in Table II. Regarding the critical current density fit for the Nb_3Sn, the one provided by the HFM programme was selected to enable comparison with results reported in the scientific literature [25]. Then for the iron yoke, the outer radius is set to 350 mm with a squared central window suitable for bladder and key technology, requiring pads with a minimum thickness of 25 mm. In particular, for the non-linear computations the soft iron ARMCO BH-curve has been used. The electromagnetic design and performance calculations for both configurations were carried out using the ROXIE [26], [27] software from CERN. The overall results of this design are summarized in Table I, and will be discussed later in Section IV-A.

III. HYBRID Nb_3Sn/NBTI DIPOLE

The second design, inspired by [3], [28], explores a Hybrid solution that represents the best compromise found between performance and cost. This design is based on a "material grading" strategy: since NbTi is only effective at lower magnetic field strengths, its use is restricted to the two outer Low-Field layers of the magnet (strand details can be found in [29]), while the two inner High-Field layers are wound with Nb_3Sn. This configuration (Fig. 1(b) seeks to maximize performance where it is most needed while limiting expenses. The bare cable specifications are listed in Table II. The same characteristics of the iron yoke of the Full-Nb_3Sn design were adopted. Regarding the critical current densities, the same fit used for the Full-Nb_3Sn was applied to the Nb_3Sn layers, while for NbTi the LHC inner cable fit was adopted [30]. The resulting performance of this

TABLE II
BARE CABLE PROPERTIES

	Full Nb_3Sn		**Hybrid Nb_3Sn/NbTi**	
	HF	**LF**	**HF**	**LF**
Material	Nb_3Sn	Nb_3Sn	Nb_3Sn	NbTi
N° strands	40	40	40	40
Strand diameter [mm]	0.85	0.7	0.85	1.065
Cu/non-Cu	1.2	1.2	1.2	1.6
Cable inner thickness [mm]	1.53	1.228	1.53	1.736
Cable outer thickness [mm]	1.658	1.437	1.658	2.222
Cable width [mm]	18.36	14.85	18.36	22.365
Insulation thickness [mm]	0.145	0.145	0.145	0.145
Quench integral [MA^2s]	30	15	30	93

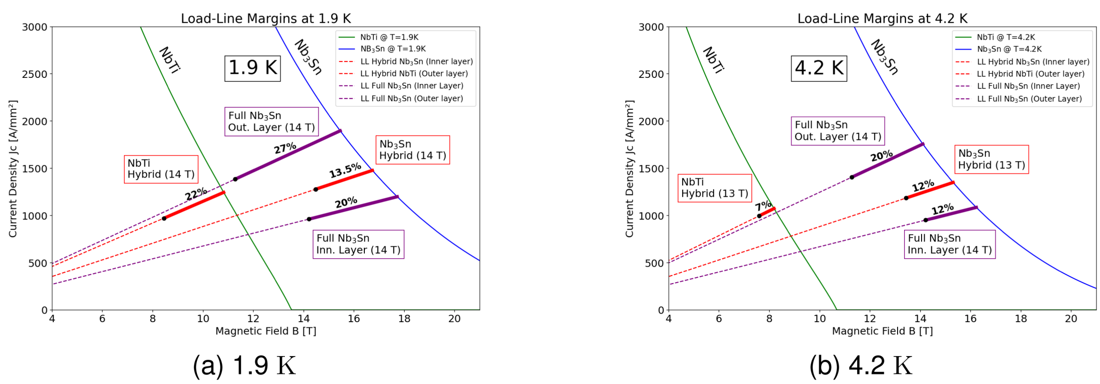

Fig. 2. Load-line margins evaluated with the ROXIE software.

Hybrid magnet is detailed in Table I and it shows a tradeoff between margin and achieved bore field that will be discussed in Section IV-A.

IV. DESIGN COMPARISON

A. Electromagnetic Margins

As shown in Fig. 2(a), at 1.9 K the Full-Nb_3Sn design meets the 20% load-line margin requirement across the entire coil. In contrast, for the Hybrid configuration, two operating scenarios must be considered. When targeting a bore field of 14 T, the Hybrid design satisfies the 20% margin only in the NbTi outer layers, while the inner Nb_3Sn layers become limiting, reducing the overall margin to 13.5%. Despite this reduction, the configuration remains attractive due to advantages in cost and potentially also in fabrication complexity. Alternatively, if the Hybrid is operated at 13 T at 1.9 K, it satisfies the 20% load-line margin requirement with margin still governed by the Nb_3Sn layers, as the NbTi remains well within its operating limits. In the FCC-hh case, this field reduction decreases the c.o.m. energy by 7%. At 4.2 K (Fig. 2(b)), the Full-Nb_3Sn design retains a margin of 12%, enabling operation at 14 T under relaxed cooling requirements. However, the Hybrid design cannot sustain 14 T at this temperature, as the NbTi outer layers exceed their short-sample performance limit. In this case, a reduced current must be used, limiting the bore field to 13 T, with a resulting load-line margin of only 7%, now dictated by the NbTi. This highlights the stronger temperature dependence of the Hybrid design and the need to carefully balance field, temperature, and stability constraints when considering this configuration.

B. Persistent Current Losses

The strand magnetization was calculated using the semi-analytical scalar model within the ROXIE code [31] and neglecting Inter-Filament (IFCC) and Inter-Strand (ISCC) Coupling Currents contribution. Losses were determined for a single current cycle, ramping from 5% to 100% of the nominal current and back down. The resulting persistent current loss for this cycle was found to be 8.5 kJ/m and 4.7 kJ/m for the Full Nb_3Sn and the Hybrid design respectively. This corresponds to a significant reduction of approximately 45% in persistent current losses for the Hybrid design relative to the Full Nb_3Sn design.

C. Quench Protection

In this study, a preliminary quench protection analysis was approached using a conservative adiabatic approximation to estimate the maximum allowable quench integral (MIITs) for the superconducting cables in the different magnet regions [33], [34]. A maximum hot-spot temperature of 300K has been considered. For the HF region both designs employ the same superconducting cable, and due to the relatively small variation in the material properties at peak magnetic field, the budget remains similar (approximately 30 MA^2s). These values were obtained under the assumption that the entire HF and LF winding operates under their peak field conditions, making this a deliberately conservative scenario. For the LF region, the MIITs budgets differ significantly due to the use of different cable technologies and geometries. The Full-Nb_3Sn design employs a smaller Nb_3Sn cable to that of the HF region, resulting in a budget of approximately 15 MA^2s. In contrast, the Hybrid configuration utilizes a NbTi cable with inherently better thermal and electrical properties, and a significantly larger cross-sectional area—nearly 50% greater than the Nb_3Sn cable used in the LF region of the Full design. These factors combine to yield a substantially higher budget of approximately 93 MA^2s for the Hybrid working at 14 T, highlighting a distinct advantage in terms of protection margin. For a short demonstrator (≅1 m), a preliminary evaluation of the current discharge during a quench event has also been performed. Assuming a protection scheme employing an external dump resistor sized to limit the maximum voltage across the terminals to 500 V, the discharge MIITs were calculated using the total stored magnetic energy of the coils. The stored energy is 1.21 MJ/m for the Full-Nb_3Sn case and 1.08 MJ/m for the Hybrid case. Under these conditions, 24 MA^2s and 29 MA^2s respectively are needed for the discharge. If the maximum voltage constraint is relaxed to 1000 V, these MIITs values are effectively halved, providing greater flexibility in the protection scheme. These preliminary findings show that for a short demonstrator the Full-Nb_3Sn design with a 1000 V maximum voltage has a time margin of 31 ms (3 MA^2s), whereas the Hybrid configuration has a time margin of 87 ms (14 MA^2s). Nonetheless, further dedicated studies to refine and optimize the quench protection system are planned.

D. Conductor Cost

The conductor is one of the cost drivers in the manufacturing of a magnet. Using updated procurement costs of 330 € /kg for NbTi and 2274 € /kg for Nb_3Sn [35], [36], the material cost advantage of the Hybrid design becomes evident. Specifically for these two designs, the saving in Nb_3Sn mass is in the order of 43%, which results in a total conductor cost of approximately 82 k€/m for the Hybrid configuration, compared to 163 k€/m for the Full-Nb_3Sn option. However, it should be noted that the Hybrid design has a reduced margin in load-line with respect to the Full-Nb_3 Sn and therefore, the reported 43% can be considered the cost needed to satisfy the 20% load-line margin requirement with 14T bore field.

E. Efficiency and Equivalent Coil Width

The *equivalent coil width* is a useful parameter for comparing different coil layouts [37]. It represents the width of a 60° sector coil that has the same cross-sectional area as the design under evaluation. This geometrical normalization provides a simple yet effective metric for assessing layout compactness. From the equivalent coil width, we derive the *layout efficiency* by calculating the bore field produced by the coil alone, removing both grading and iron contributions [37]. This approach provides a clearer understanding of the conductor performance and its utilization within the magnet design. Our benchmark value for the coil efficiency is 6.63×10^{-4} Tmm/A, result that comes from the efficiency of a 60° sector coil, without iron and grading [37]. Using this reference, the Full-Nb_3Sn layout achieves 98% of the benchmark, while the Hybrid Nb_3Sn/NbTi configuration reaches 97.1%. These values indicate that both coil layouts are highly efficient in terms of conductor utilization, with only a marginal difference between them. The Hybrid Nb_3Sn/NbTi configuration, despite incorporating a lower-performance material in the LF region, achieves over 97% of the benchmark efficiency. This observation suggests that there may be room for further optimization of the Hybrid layout. In particular, a reduction in the number of strands in the NbTi cable could be explored as a strategy to decrease the total cable cross-sectional area and, consequently, the equivalent coil width. Such an adjustment would have the potential to improve the normalized layout efficiency, while offering additional benefits in terms of material cost reduction. Given the significantly higher MIITs budget available in the LF region of the Hybrid design a slight reduction in the copper volume would likely not compromise quench protection. Instead, it may allow a more cost-effective and compact implementation, especially relevant for large-scale magnet production. Future iterations of the Hybrid concept could investigate this trade-off more quantitatively, balancing layout efficiency, protection margin, and economic considerations.

F. Conductor Stress

For high-field accelerator magnets with a bore field of 14T, the conductor stress could approach the 150MPa HFM threshold. This makes a detailed structural design crucial for project feasibility. We initiated this work by estimating the peak accumulation of azimuthal stress in the mid-plane and radial stress using the analytical model proposed in [38]. The agreement between this model and the FEM analysis for the peak azimuthal and radial stresses in D20, a relatively similar design, is within 20% [38]. The results for our designs, reported in Table I, are comparable to those of similar existing magnets such as MDPCT1 and D20. This comparison strengthens our confidence in the feasibility of the magnet mechanical structure. However, these results must be validated through FEM analysis, which will be carried out in collaboration with INFN Genova.

V. Conclusion

This study presented a comparative analysis of two design options for a four-layer high-field dipole magnet: a Full-Nb_3Sn configuration and a Hybrid Nb_3Sn/NbTi layout. While only the Full-Nb_3Sn magnet is capable of reaching the target bore field of 14 T with 20% load-line margin, the Hybrid configuration shows promising characteristics in terms of cost reduction, splice complexity and persistent current losses. These trade-offs make it a viable alternative for further exploration, especially in applications where slightly reduced performances are acceptable. However, the Full-Nb_3Sn design is selected for the fabrication of a short model at the upcoming *IRIS facility* [39], [40], [41], [42], [43] located at the *Laboratory of Accelerators and Applied Superconductivity* in INFN Milan in the next years. This will serve as a technological demonstrator for future high-field magnets intended for post-LHC collider applications. The next steps in the project will include a detailed quench protection and structural analysis, which is essential to ensure operational safety and reliability. These activities will be key to validating the design and preparing for future scaling toward a full-length prototype suitable for accelerator integration.

REFERENCES

[1] A. Abada et al., "FCC-hh: The hadron collider," *Eur. Phys. J. Spec. Top.*, vol. 228, pp. 755–1107, 2019, doi: 10.1140/epjst/e2019-900087-0.

[2] A. Haziot, "Nb_3Sn/NbTi hybrid concepts in block for high field dipole magnets," presented at the MT 29 2025, Boston, MA, USA, Jul. 1-6, 2025.

[3] J. Á. Garcıá-Matos, C. M. Jardim, F. Toral, J. C. Perez, and E. Todesco, "Magnetic design of a 14 T common coil demonstrator magnet (DAISY)," *IEEE Trans. Appl. Supercond.*, vol. 35, no. 5, Aug. 2025, Art. no. 4002605, doi: 10.1109/TASC.2025.3537069.

[4] F. Toral, "Exploring hybrid designs for a 14 T common coil demonstrator magnet (DAISY)," presented at the MT 29 2025, Boston, MA, USA, Jul. 1-6, 2025.

[5] Z. Hou et al., "Conceptual mechanical structure analysis of a 16 T canted cosine theta (CCT) magnet," *IEEE Trans. Appl. Supercond.*, vol. 34, no. 5, Aug. 2024, Art. no. 4001204, doi: 10.1109/TASC.2023.3346858.

[6] I. Novitski et al., "Development and test of a large-aperture Nb_3Sn cos-theta dipole coil with stress management," *IEEE Trans. Appl. Supercond.*, vol. 34, no. 5, Aug. 2024, Art. no. 4001305, doi: 10.1109/TASC.2023.3344424.

[7] E. Todesco, "Status and perspectives of high field magnets for particle accelerators," *IEEE Trans. Appl. Supercond.*, vol. 35, no. 5, Aug. 2025, Art. no. 4003914, doi: 10.1109/TASC.2025.3558196.

[8] "High field magnet website," Accessed: Jul. 18, 2025. [Online]. Available: https://hfm.web.cern.ch/

[9] R. U. Valente et al., "Design of a four-layer Nb_3Sn cos-theta dipole in the CERN high field magnet R&D program," *IEEE Trans. Appl. Supercond.*, vol. 35, no. 5, Aug. 2025, Art. no. 4100105, doi: 10.1109/TASC.2024.3515962.

[10] R. Valente et al., "Electromagnetic and mechanical study for the Nb_3Sn cos-theta dipole model for the FCC," *IEEE Trans. Appl. Supercond.*, vol. 30, no. 4, Jun. 2020, Art. no. 4001905, doi: 10.1109/TASC.2020.2972219.

[11] A. Pampaloni et al., "Preliminary design of the Nb_3Sn cosθ short model for the FCC," *IEEE Trans. Appl. Supercond.*, vol. 31, no. 5, Aug. 2021, Art. no. 4900905, doi: 10.1109/TASC.2021.3061334.

[12] R. U. Valente et al., "Update on the electromagnetic design of the Nb_3Sn cos-theta dipole model for FCC-hh," *IEEE Trans. Appl. Supercond.*, vol. 32, no. 4, Jun. 2022, Art. no. 4001005, doi: 10.1109/TASC.2022.3152100.

[13] R. U. Valente, "Electromagnetic design optimization of the 12 T cos-theta dipole model for the FCC," Ph.D. dissertation, Sch. Accel. Phys., La Sapienza Univ Rome, Rome, Italy, 2022, [Online]. Available: https://hdl.handle.net/11573/1668577

[14] R. U. Valente et al., "Study of superconducting magnetization effects and 3D electromagnetic analysis of the Nb_3Sn cosθ short model for FCC," *IEEE Trans. Appl. Supercond.*, vol. 31, no. 5, Aug. 2021, Art. no. 4002205, doi: 10.1109/TASC.2021.3059981.

[15] S. Burioli et al., "Cos-theta dipole model for the FCC-hh at CERN," 2021. [Online]. Available: http://www.lnf.infn.it/sis/preprint/getfilepdf.php?filename=INFN-22-01-GE.pdf

[16] A. Pampaloni et al., "Mechanical design of FalconD, a Nb_3Sn cos-theta short model dipole for the FCC," *IEEE Trans. Appl. Supercond.*, vol. 32, no. 6, Sep. 2022, Art. no. 4000605, doi: 10.1109/TASC.2022.3149679.

[17] F. Levi et al., "Updates on the mechanical design of FalconD, a Nb_3Sn cosθ short model dipole for FCC-hh," *IEEE Trans. Appl. Supercond.*, vol. 33, no. 5, Aug. 2023, Art. no. 4000805, doi: 10.1109/TASC.2023.3241832.

[18] R. U. Valente et al., "Optimization of electromagnetic design after winding tests for the Nb_3Sn cos-theta dipole model for FCC-hh," *IEEE Trans. Appl. Supercond.*, vol. 33, no. 5, Aug. 2023, Art. no. 4601107, doi: 10.1109/TASC.2023.3246421.

[19] R. U. Valente et al., "Status on the development of the Nb_3Sn 12 T falcon dipole for the FCC-hh," *IEEE Trans. Appl. Supercond.*, vol. 34, no. 3, May 2024, Art. no. 4900405, doi: 10.1109/TASC.2023.3338166.

[20] S. Farinon et al., "Advancements in Nb_3Sn 12 T cos-theta dipole development for next-generation accelerators: The INFN-CERN collaboration on the FalconD project," *IEEE Trans. Appl. Supercond.*, vol. 35, no. 5, Aug. 2025, Art. no. 4001905, doi: 10.1109/TASC.2024.3520944.

[21] R. U. Valente, "Winding challenges and solutions in the INFN falcon dipole project," presented at the MT 29 2025, Boston, MA, USA, Jul. 1-6, 2025.

[22] P. Ferracin et al., "The HL-LHC Low-β quadrupole magnet MQXF: From short models to long prototypes," in *IEEE Trans. Appl. Supercond.*, vol. 29, no. 5, Aug. 2019, Art. no. 4001309, doi: 10.1109/TASC.2019.2895908.

[23] S. Caspi et al., "LBNL cos-theta Nb_3Sn dipole magnet D20," in *Nb_3Sn Accelerator Magnets. Particle Acceleration and Detection*, D. Schoerling and A. Zlobin Eds. Cham, Switzerland: Springer, 2019, doi: 10.1007/978-3-030-16118-7_6.

[24] A. V. Zlobin et al., "Development and first test of the 15 T Nb_3Sn dipole demonstrator MDPCT1," *IEEE Trans. Appl. Supercond.*, vol. 30, no. 4, Jun. 2020, Art. no. 4000805, doi: 10.1109/TASC.2020.2967686.

[25] C. S. Hopkins, "J_c scaling and data fitting for Nb_3Sn wires," HFM-MDP Forum, Feb. 20, 2025. [Online]. Available: https://indico.cern.ch/event/1510243/contributions/6355907/attachments/3018928/5325624/Jc%20scaling%20Feb%202025.pdf

[26] S. Russenschuck, "ROXIE: routine for the optimization of magnet X-sections, inverse field calculation and coil end design," *CERN*, Geneva, 1999, doi: 10.5170/CERN-1999-001.

[27] S. Russenschuck, *Field Computation for Accelerator Magnets: Analytical and Numerical Methods for Electromagnetic Design and Optimization*. New York, NY, USA: Wiley, 2011.

[28] S. Caspi et al., "Design and construction of a hybrid-Nb_3Sn, NbTi-dipole magnet," *IEEE Trans. Appl. Supercond.*, vol. 7, no. 2, pp. 547–550, Jun. 1997, doi: 10.1109/77.614562.

[29] O. S. Bruning et al., "LHC design report," *CERN*, Geneva, 2004, doi: 10.5170/CERN-2004-003-V-1.

[30] L. Bottura, "A practical fit for the critical surface of NbTi," *IEEE Trans. Appl. Supercond.*, vol. 10, no. 1, pp. 1054–1057, Mar. 2000, doi: 10.1109/77.828413.

[31] M. Aleksa, S. Russenschuck, and C. Vollinger, "Magnetic field calculations including the impact of persistent currents in superconducting filaments," *IEEE Trans. Magn.*, vol. 38, no. 2, pp. 825–828, Apr. 2002.

[32] A. Haziot, "NbTi Hybrid Block Coil Designs - The BOND Case -, slide 18," (n.d.). [Online]. Available: https://indico.cern.ch/event/1524821/contributions/6415048/attachments/3044182/5379574/Pres%20AH%2025.04.03%20nbti.pdf

[33] M. N. Wilson, *Superconducting Magnets*. Oxford, U.K.: Oxford Science Publication, 1983.

[34] E. Todesco, "Masterclass - design of superconducting magnets for particle accelerators, unit 12 - protection principles," Accessed: Sep. 08, 2025. [Online]. Available: https://indico.cern.ch/event/926967/attachments/2096737/4758147/12.pdf

[35] B. Caiffi et al., "Challenges and perspectives of the superconducting magnets for the muon collider storage ring," *IEEE Trans. Appl. Supercond.*, vol. 35, no. 5, Aug. 2025, Art. no. 4002007, doi: 10.1109/TASC.2025.3529424.

[36] L. Bottura et al., "Magnets timeline, cost and R&D plan," in *Proc. IMCC MuCol Annu. Meeting*, Hamburg, Germany, 2025, pp. 12–16.

[37] E. Todesco, "Masterclass - design of superconducting magnets for particle accelerators, unit 4 - how to generate dipole and quadrupole fields with current lines," Accessed: Jul. 19, 2025. [Online]. Available: https://indico.cern.ch/event/915752/attachments/2047343/4441872/Chapter4p.pdf

[38] E. Todesco et al., "Analytical estimates of stress in superconducting dipole magnets for particle accelerators," *Supercond. Sci. Technol*. vol. 38, no. 6, 2025, Art. no. 065004, doi: 10.1088/1361-6668/add424.

[39] "INFN IRIS website," Accessed: Jul. 18, 2025. [Online]. Available: https://iris.infn.it/it

[40] L. Rossi et al., "Progress in the IRIS project in italy," presented at the ASC 2024, Salt Lake City, UT, USA, Sep. 1-6, 2024.

[41] "Next generation EU website," Accessed: Jul. 18, 2025. [Online]. Available: https://next-generation-eu.europa.eu/recovery-and-resilience-facility_en

[42] L. Rossi et al., "IRIS-The italian research infrastructure on applied superconductivity for particle accelerators and societal applications," *J. Phys.: Conf. Ser.*, vol. 2687, 2024, Art. no. 092012, doi: 10.1088/1742-6596/2687/9/092012.

[43] L. Rossi et al., "IRIS-A new distributed research infrastructure on applied superconductivity," *IEEE Trans. Appl. Supercond.*, vol. 34, no. 3, May 2024, Art. no. 9500309, doi: 10.1109/TASC.2023.3341984.